Available online at www.sciencedirect.com

SciVerse ScienceDirect

Ceramics International 39 (2013) 555–561

CERAMICS INTERNATIONAL

www.elsevier.com/locate/ceramint

Synthesis, dielectric and relaxation behavior of lead free NBT–BT ceramics

S. Shanmuga Sundari[a], Binay Kumar[b], R. Dhanasekaran[a,*]

[a]Crystal Growth Centre, Anna University, Chennai 600025, Tamil Nadu, India
[b]Crystal Lab, Department of Physics and Astrophysics, University of Delhi, Delhi 110007, India

Received 24 May 2012; received in revised form 21 June 2012; accepted 21 June 2012
Available online 29 June 2012

Abstract

The $0.94(Na_{0.5}Bi_{0.5}TiO_3)$–$0.06BaTiO_3$ ceramics have been prepared by the conventional solid state reaction method. Structural analysis of the prepared ceramic was made by means of room temperature XRD, FT-IR and Raman spectra. The formation of perovskite structure is confirmed by XRD and Raman studies. The dependence of dielectric constant on temperature for various frequencies (100 Hz–1.2 MHz) has been determined. The diffuse transition is observed in the variation of dielectric constant and it provides evidence for the relaxor characteristics. The relaxation mechanism of the prepared ceramic is also discussed in detail by using Debye, V–F and Power law relations and the suitable model was predicted by means of goodness of parameter. This is the first time the relaxation process is discussed for the lead free system to the best of our knowledge. High piezoelectric properties with $d_{33}=206$ pC/N are observed in the present system.

Keywords: A. Solid state reaction; C. Dielectric properties; C. Piezoelectric properties; D. Perovskites

1. Introduction

Devices using dielectric and piezoelectric properties of ferroelectric materials are receiving a continuous attraction. The high performance piezoelectric materials are effectively used in actuators, sensors, and other transducer applications. The perovskite relaxor ferroelectric materials have opened up new opportunities not only in current acoustic transducers, but also in exploration of new applications, such as medical ultrasonics, non-destructive detection, marine seismic exploration and energy harvesting [1,2]. The piezoelectric coefficient (d_{ij}) and its temperature dependence are the critical parameters for the piezoelectric actuator applications. Lead oxide-based perovskites exhibit some of the highest piezoelectric coefficients of known compounds and are now widely used in these applications [1]. The lead based materials like PZN-PT and PMN-PT have shown superior piezoelectric strain coefficients ($d_{33}=1500$ pC/N) and electromechanical coupling factors ($k_{33}=0.92$) [3–5]. The toxicity of lead made these materials expelled from commercial applications and materials concerning the environmental safety regulations. The comparable piezoelectric properties to that of PZT are also found in lead free materials when they are prepared in Morphotropic Phase Boundary (MPB) [6]. The superior piezoelectric properties are as a result of MPB which separates the tetragonal and rhombohedral phases. Because the polar vector of domains changes orientation spontaneously when the ferroelectric phase boundary is crossed, for compositions close to the boundary it is quite easy for an electric field to tilt the polar vector [7]. Coupling between the two equivalent energy states, i.e., the tetragonal and rhombohedral phases, allows the optimum domain reorientation during the poling process [8].

The bismuth based materials seem to be an attractive candidate for lead free materials. In this context, sodium bismuth titanate $Na_{0.5}Bi_{0.5}TiO_3$ (NBT) was considered to be one of the most promising aspirants to replace lead based materials [9,10]. The high coercive field of NBT moved the attraction towards its solid solution with

*Corresponding author. Tel./fax: +91 44 22358317.
E-mail addresses: rdcgc@yahoo.com, rdhanasekaran@annauniv.edu (R. Dhanasekaran).

0272-8842/$36.00 © 2012 Elsevier Ltd and Techna Group S.r.l. All rights reserved.
http://dx.doi.org/10.1016/j.ceramint.2012.06.063

$PbTiO_3$ [11], $SrTiO_3$ [12], $La_2(TiO_3)_3$ [13], $KNbO_3$ [14] and $BaTiO_3$ [15]. Among these NBT-based systems, $(1-x)(Na_{1/2}Bi_{1/2})TiO_3$–$xBaTiO_3$ is more focused. Takenaka et al. [15] pointed out that at room temperature it has a rhombohedral (F_α)–tetragonal (F_β) Morphotropic Phase Boundary (MPB) at $x=0.06$–0.07 where the system shows outstanding piezoelectric and dielectric properties of all the lead free ceramic resources.

In the present work, the $0.94(Na_{0.5}Bi_{0.5}TiO_3)$–$0.06(BaTiO_3)$ (NBT–BT) lead free ceramics were prepared by the conventional solid state reaction method and their structural, temperature dependence of dielectric properties and piezoelectric properties were studied systematically. There are few reports on the topic of the Raman spectroscopic study of NBT [16–18] and NBT-based materials [19,20]. The present paper reports the results of the room temperature Raman scattering and infrared studies of NBT–BT ceramic. A detailed discussion about the dependence of dielectric constant on temperature of NBT–BT ceramics was made. To understand the relaxation behavior of the prepared ceramics three different methods namely Debye, Vogel–Fulcher and Power law were used.

2. Experimental Techniques

The solid state reaction method was used to prepare the NBT–BT ceramics. High purity (99.9%) Na_2CO_3, $BaCO_3$, Bi_2O_3 and TiO_2 were used as initial precursors. The oxide and carbonates were weighed according to the composition of $0.94(Na_{0.5}Bi_{0.5}TiO_3)$–$0.06(BaTiO_3)$. The carbonates and oxides were mixed homogeneously in ethanol medium and calcined at 850 °C for 4 h. The calcined powders were reground and mixed with binder (polyvinyl alcohol). After drying, pellets of the size 19 mm diameter and 1 mm thickness were made by applying pressure of 300 MPa. The prepared discs were sintered at 1200 °C for 4 h. The shrinkage of the prepared ceramics along the radial and axial direction was 17.6% and 24.1%, respectively, and no shape change is observed. The obtained ceramics were finely ground and subjected to powder XRD in the range of 10–80° of 2θ with the step angle of 0.02° and step time 1 s using PANalytical diffractometer (CuK_α radiation) to confirm the phase formation and crystalline nature. Surface morphology of the gold coated sintered samples was studied by scanning electron microscopy (S-3400). The FT-IR spectrum of the specimen was recorded using Perkin Elmer spectrum RX-1 by the KBr method in the wave number range 400–4000 cm^{-1} and the Raman spectra was recorded using Bruker instrument. The variation of dielectric constant with temperature at different frequencies (100 Hz–2 MHz) was studied from room temperature to 350 °C using Agilent E4980A impedance analyser. Ceramics were poled by applying a field 25 kV/cm at room temperature for 20 min. The piezoelectric coefficient d_{33} (pC/N) was measured using Piezometer (PM300, Piezotest).

3. Results and discussion

Fig. 1 shows the refined XRD pattern of the NBT–BT ceramics in the 2θ range 10–80°. The profile fit was carried out by using FullProf programme. The Bragg peaks were modeled with pseudo-Voigt function. The resulting Profile R-Factor (R_p) and Chi-Square (χ^2) were 21.4 and 1.4, respectively. The refinement results show pure perovskite phase and no secondary phases are observed implying that Ba^{2+} has diffused into the NBT lattices to form a solid solution [21]. The structure of NBT–BT ceramic has cubical symmetry with the space group $pm-3m$. The lattice parameters are $a=b=c=3.901$ Å and $\alpha=90°$. Fig. 2 displays the SEM micrograph of a surface of NBT–BT ceramics. It shows that the prepared ceramic is relatively dense, pore free and homogeneous. The grain size is about 1.6 μm. The smaller grain size may be due to the substitution of Ba^{2+} which inhibits the grain growth [22].

The FT-IR spectrum of NBT–BT ceramic is recorded at room temperature in the range of 400–4000 cm^{-1} and it is shown in Fig. 3. The bands at 658 $cm^{-1}$and 847 cm^{-1} are corresponding to the bending vibration of Bi–O units in $[BiO_3]$ and $[BiO_6]$ polyhedral units, respectively, and this may arise due to the inter-polyhedral vibration. The presence of bands at 1423 cm^{-1} and 1628 cm^{-1} are due to the stretching vibration of BO_6, i.e., TiO_6 in perovskite structure and this asymmetric stretching vibration changes the bond length of Ti–O bond along the c-axis and confirms the presence of oxygen group [23].

The deconvoluted Raman spectrum of prepared NBT–BT ceramic is displayed (Fig. 4). The deconvolution was performed on the basis of 4 Gaussian–Lorentzian modes. The spectrum is consistent with previous reports [19,20,24]. The broad bands in the spectrum are due to the creation of disorder in the lattice structure by the A-site ion and due to the overlapping of Raman modes. The A-site distortion may be explained in the following manner. The atomic mass of

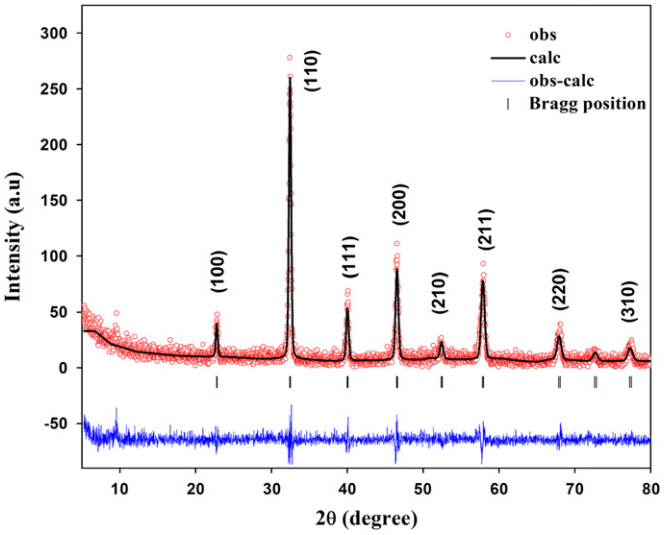

Fig. 1. X-ray diffraction pattern of NBT–BT ceramics and Rietveld profile fit also shown.

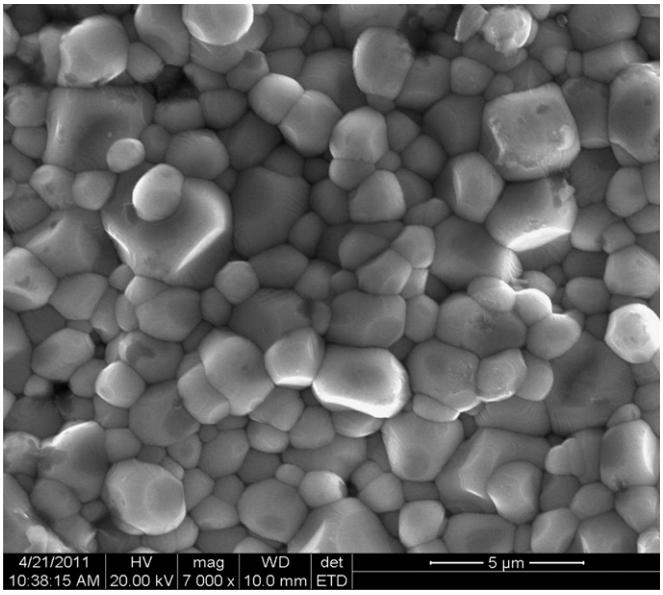

Fig. 2. SEM micrograph of NBT–BT ceramic.

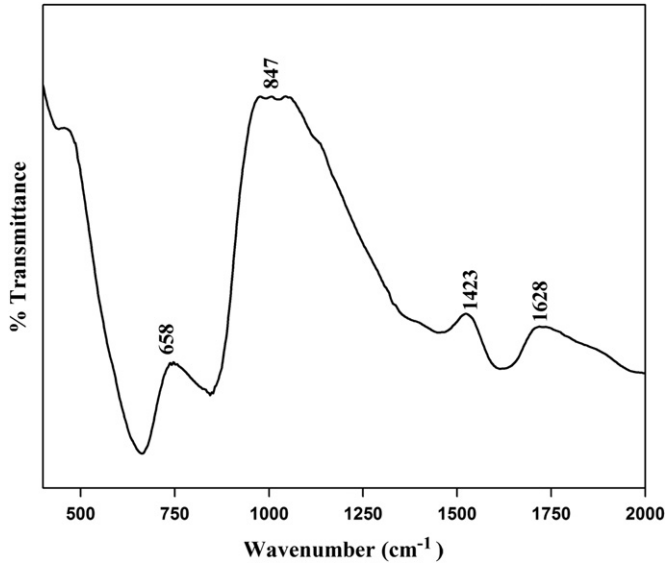

Fig. 3. FT-IR spectra of the NBT–BT ceramic.

the Ba^{2+} is in between the mass of Na^{+} and Bi^{3+} ions and the ionic radius of Ba^{2+} is larger when compared to that of Bi^{3+} and Na^{+}. So when the substitution of Ba^{2+} in the NBT lattice will create the A-site distortion in the perovskite structure, four bands are clearly visible around 269 cm^{-1}, 539 cm^{-1}, 613 cm^{-1} and 822 cm^{-1}. The band at 269 cm^{-1} is very sensitive to any structural transitions. It is dominated by A_1 mode vibrations and it corresponds to the to the vibration modes of Na–O and Ti–O bonds [19,20]. The high frequency bands near 539 and 613 cm^{-1} are well known for NBT-based ceramics and are attributed to the vibration of TiO_6 namely stretching and breathing vibration of oxygen octahedrons [20]. The 822 cm^{-1} band can be correlated to the presence of oxygen vacancies, while their intensity yields

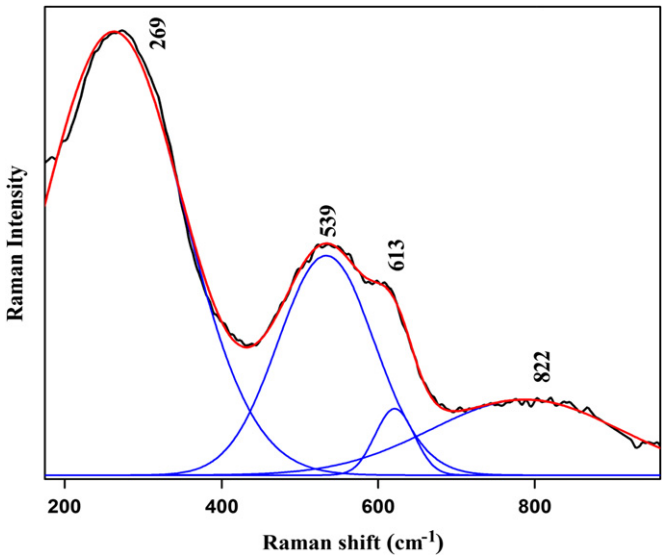

Fig. 4. Raman spectra of NBT–BT ceramic.

the vacancy concentration [25]. This region can be linked to the A_1 (LO) and E (LO) overlapping bands. Due to the high mass of the bismuth atom, the Bi–O band will fall at a very low frequency and was not observed in our experimental conditions.

The variations of real part (ε') and imaginary part (ε'') of dielectric constant and as a function of temperature for various frequencies (100–1.2 MHZ) are shown in Fig. 5(a) and (b), respectively. The dielectric response exhibits the diffuse phase transition and it is observed by the shift of dielectric maxima (ε_m') towards higher temperatures with increasing frequency. A similar diffuse phase transition has been observed in many ABO_3 type perovskites and bismuth layer-structured compounds [26,27]. There are two dielectric anomalies existing in the present system as in other relaxor ferroelectric materials at T_d and T_m, where T_d corresponds to transition from ferroelectric to anti-ferroelectric state and T_m corresponds to the anti-ferro-electric to paraelectric state. The dielectric peaks at T_d exhibit strong frequency dependence, implying that ceramics undergo a relaxor phase transition at T_d and it is the indication of stability of ferroelectric domains. The dielectric peaks at T_m for the ceramics are relatively broad, suggesting that the phase transition at T_m is a diffuse phase transition. In NBT–BT ceramic, Na^{+}, Bi^{3+} and Ba^{2+} ions are randomly distributed in the 12-fold coordination sites, so the observed diffuse phase transition behavior at T_m is reasonably attributed to the disordering of A-site cations [22]. The non-stoichiometric defect states also influence the dielectric function of a material [28]. The values of T_d and T_m in the present system are low when compared to other lead free ceramics [21,26,29,30], which favors their possible applications in the lead free world. As discussed by Chu et al. [31], the improvement of piezoelectric properties depends upon the sufficient reorientation of 90° domains. Lower T_d means the lower stability, which favors the easy reorientation of 90° domains. Thus the materials with

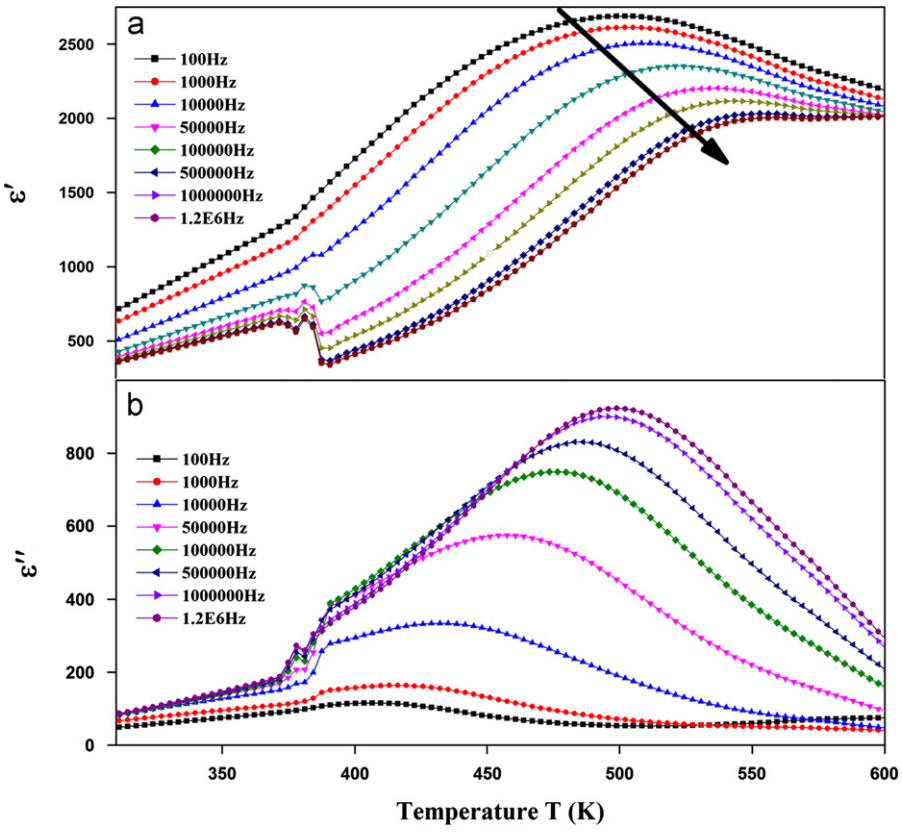

Fig. 5. Variation of (a) real part of dielectric constant (ε') and (b) imaginary part of dielectric constant (ε'') as a function of temperature for various frequencies.

Table 1
The values of T_d and T_m of the present work and for some lead free materials.

Sample	Present work	NBT–BT [21]	NBT–KBT–BT [26]	NBT–NBZN [28]	NBT–KBT [29]
T_d at 1 kHz (K)	378	463	478	483	433
T_m at 1 kHz (K)	496	658	573	588	605

lower T_d show better piezoelectric properties. The values of T_d and T_m at 1 kHz of the prepared ceramic and reported values of other lead free ceramics are tabulated in Table 1 for comparison.

The diffuseness of the relaxor ferroelectrics can be further explained by fitting the dielectric data with the modified Curie–Weiss law [32]

$$\frac{1}{\varepsilon'} - \frac{1}{\varepsilon'_m} = \frac{1}{k(T-T_m)^{\gamma}} \quad (1)$$

where ε'_m is the dielectric maximum at the transition temperature (T_m), k is a constant, T is the absolute temperature and γ is the degree of diffuseness. It is well known that γ is equal to 2 for typical relaxor ferroelectrics and 1 for normal ferroelectrics. Fig. 6 shows the graph between $\ln(1/\varepsilon' - 1/\varepsilon'_m)$ and $\ln(T-T_m)$ at 1 kHz. By fitting the experimental data to Eq. (1) the γ value is found 1.7 which fell into the prescribed region. The diffusivity γ corresponds to a very broad relaxation and higher disorder.

The Debye medium is a classic dielectric. In the Debye medium the dipoles are thermally activated and there will not be any interaction between the dipoles. Hence the relaxation time (τ) can be said to obey the Arrhenius law [33]

$$\omega = \omega_0 \exp(-E/k_B T_m) \quad (2)$$

where $\tau = 1/\omega$, k_B is the Boltzmann constant and the ω_0 is the attempt frequency of a molecule (Debye frequency), E is the activation energy. But the experimental results proved that not all the dipoles are free and there may be an interaction between the dipoles. These interactions make the dipoles to freeze at a particular temperature called T_f. This inadequacy of Debye model is taken into account in Vogel–Fulcher (V–F) model and it is given by [34]

$$\omega = \omega_0 \exp(-E/k_B(T_m - T_f)) \quad (3)$$

where T_f is the freezing temperature and also the temperature of static dielectric constant maximum.

Fig. 7 shows the fitting to the Debye and V–F model and the values are tabulated in Table 2. In Eq. (3) if T_f equals to zero, it becomes Eq. (2) and T_m becomes the Curie temperature in the case of ferroelectrics regardless of the value of T_f. As discussed by Cheng et al. [35] V–F model fails to differentiate ferroelectrics and relaxor ferroelectrics. To overcome this lack of V–F model, Cheng et al. [35] proposed a power law

$$\omega = \omega_0 \exp(-E/k_B T_m)^p \quad (4)$$

where 'p' is a constant. When p equals to 1 Eq. (4) becomes Eq. (2) and when 'p' tends to infinity and T_m tends to T_c it explains the ferroelectric behavior of the materials. The relaxation process is very week for ferroelectrics. For the relaxor ferroelectric materials the 'p' value should be greater than 1 and the value further increases as the dielectric relaxation decreases hence the lower value of 'p' corresponds to the stronger relaxation [36,37]. Thus the relaxation process is characterized by the value of 'p'. The experimental values are fitted to Eqs. (2)–(4) using Levenberg–Marquardt non-linear fit and it is shown in Fig. 7 and goodness of fit parameter in terms of χ^2 is given in Table 2. The value of ω_0, E and 'p' for the prepared NBT–BT ceramic is given in Table 2.

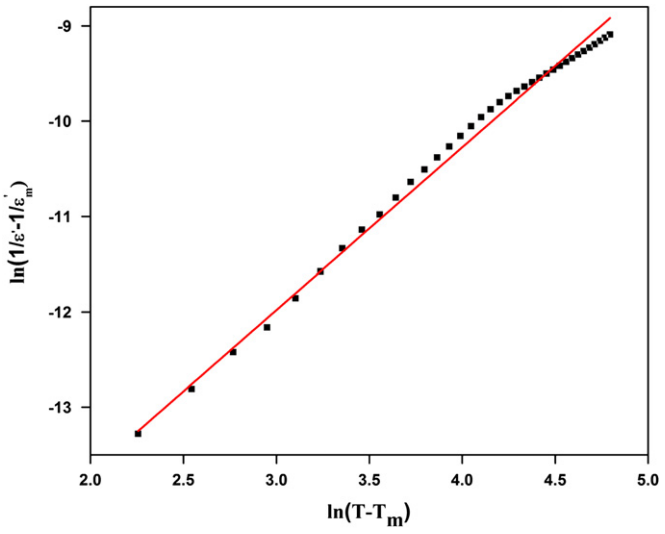

Fig. 6. Dielectric permittivity data fitted with modified Curie–Weiss law for NBT–BT ceramic at 1 kHz frequency.

Based on the reduced χ^2 value it seems that the power model gives the best fit to the present data. The attempt frequency ω_0 gives the knowledge about the size and interaction between the polar clusters [38]. For large volume of polar clusters and stronger interaction the value of ω_0 will be small. That makes the T_m to shift towards higher temperature side and a more broadening of the dielectric peaks. The value of p determines the degree of relaxation and hence the rate of growth of polar clusters. More the relaxation, slower is the rate of growth of polar clusters. For the prepared ceramics the relaxation is more when compared to the reported values [39].

To measure the piezoelectric constant (d_{33}) the electroded sample were poled at 2.5 kV/mm for 20 min. The observed d_{33} value is 206 pC/N. The controlled domain movement results in the high d_{33} value when compared to the reported values of other NBT–BT ceramics [13,21,40].

4. Conclusions

In MPB composition the NBT–BT ceramics were prepared by the conventional solid state reaction method. The formation of ABO_3 perovskite structure is confirmed by the XRD analysis. The FT-IR and Raman analyses confirm the same and the broad bands emphasize the A-site lattice

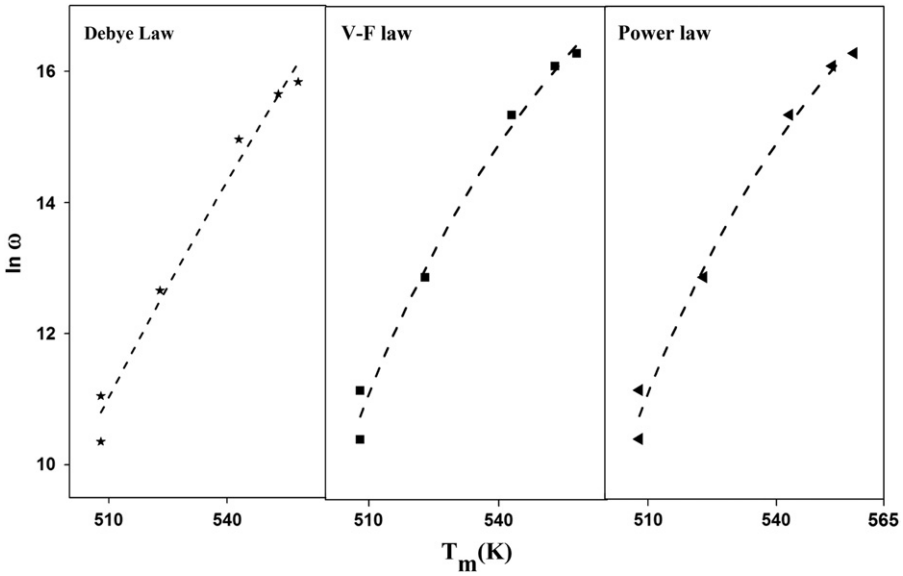

Fig. 7. Fitting of Debye, V–F and Power law to the dielectric relaxation data of the NBT–BT ceramic.

Table 2
Fitting parameters of Debye, V–F, Power law and reduced χ^2 for the NBT–BT ceramic.

Method	Attempt frequency ω_0 (Hz)′	Activation energy E (eV)	Freezing temperature (T_f) (K)	p	Reduced χ^2
Debye	2.5×10^{30}	2.6	–	–	0.119
Vogel–Fulcher	1.4×10^{11}	0.12	415.39	–	0.099
Power law	6.1×10^{8}	0.06	–	8.53	0.096

disorder. The dielectric behavior was measured from room temperature to 350 °C in the frequency range 20 Hz–1.2 MHz. From that the strong frequency dependence of T_d is observed. The shift in T_m toward higher temperature side as a function of frequency was observed suggesting the relaxor ferroelectric nature of NBT–BT ceramic. The experimental data have been used to calculate the activation energy, Debye frequency and freezing temperature using the Debye, Vogel–Fulcher and Power law models. The values are in acceptable range and also they clearly explained the presence of strong relaxation characteristics of the prepared sample. From the goodness of fit parameter it is concluded that the power law model is more suitable to explain the relaxation process of the prepared ceramics. Due to the strong relaxation, high piezoelectric coefficient (d_{33} = 206 pC/N) is observed in the prepared sample.

Acknowledgments

The authors are thankful to the UGC-New Delhi, India for the financial support. One of the authors SSS acknowledge the DST, Government of India for the award of INSPIRE fellowship.

References

[1] Ye Zuo-Guang, Hand Book of Advanced Dielectric, Piezoelectric and Ferroelectric Materials, Woodhead, England, 2008.
[2] P.K. Panda, Review: environmental friendly lead-free piezoelectric materials, Journal of Materials Science 44 (2009) 5049.
[3] J. Kuwata, K. Uchino, S. Nomura, Dielectric and piezoelectric properties of $0.91Pb(Zn_{1/3}Nb_{2/3})O_3$–$0.09PbTiO_3$ single crystals, Japanese Journal of Applied Physics 21 (Part 1) (1982) 1298.
[4] B.K. Singh, B. Kumar, Impedance analysis and high temperature conduction mechanism of flux grown $Pb(Zn_{1/3}Nb_{2/3})0.91Ti_{0.09}O_3$ single crystals, Crystal Research and Technology 45 (2010) 1003.
[5] J. Bubesh Babu, G. Madeswaran, Chandra Prakash, R. Dhanasekaran, Growth, structural phase transition and ferroelectric properties of $Pb[(Zn_{1/3}Nb_{2/3})0.91Ti_{0.09}]O_3$ single crystals, Journal of Crystal Growth 292 (2006) 399.
[6] Y. Saito, H. Takao, T. Tani, T. Nonoyama, K. Takatori, T. Homma, Lead free piezoceramics, Nature 432 (2004) 84.
[7] Eric Cross, Material science: lead free at Last, Nature 432 (2004) 24.
[8] Shujun Zhang, Ru Xia, T.R. Shrout, Lead free piezoelectric ceramics vs PZT?, Journal of Electroceramics 19 (2007) 251
[9] G.A. Smolenskii, V.A. Isupov, A.I. Agranovskaya, N.N. Krainik, New ferroelectrics of complex composition, Soviet Physics—Solid State 2 (1961) 2651.
[10] J. Bubesh Babu, G. Madeswaran, Ming He, D.F. Zhang, X.L. Chen, R. Dhanasekaran, Inhomogeneity issues in the growth of $Na_{1/2}Bi_{1/2}TiO_3$–$BaTiO_3$ single crystals, Journal of Crystal Growth 310 (2008) 467.
[11] K. Sakata, T. Takenaka, Y. Naitou, Phase relations, dielectric and piezolelectric properties of ceramics in the system $(Bi_{0.5}Na_{0.5})TiO_3$–$PbTiO_3$, Ferroelectrics 131 (1992) 219.
[12] K. Sakata, Y. Masuda, Ferroelectric and anti-ferroelectric properties of $(Na_{0.5}Bi_{0.5})TiO_3$–$SrTiO_3$ solid solution ceramics, Ferroelectrics 5 (1974) 347.
[13] A. Herabut, A. Safari, Processing and electrochemical properties of $(Bi_{0.5}Na_{0.5})_{(1-1.5X)}La_XTiO_3$ Ceramics, Journal of the American Ceramic Society 80 (1997) 2954.
[14] G. Fan, W. Lu, X. Wang, F. Liang, J. Xiao, Phase transition behaviour and electrochemical properties of $(Na_{1/2}Bi_{1/2})TiO_3$–$KNbO_3$ lead free piezoelectric ceramics, Journal of Physics D: Applied Physics 41 (2008) 35403.
[15] T. Takenaka, K.I. Maruyama, K. Sakata, $(Bi_{1/2}Na_{1/2})TiO_3$–$BaTiO_3$ system for lead free piezoelectric ceramics, Japanese Journal of Applied Physics 30 (9B) (1991) 2236.
[16] I.G. Siny, T.A. Smirnova, T.V. Kruzina, The phase transition dynamics in $Na_{1/2}Bi_{1/2}TiO_3$, Ferroelectrics 124 (1991) 207.
[17] M. Zhang, J.F. Scott, I.A. Zvirgds, Raman spectroscopy of $Na_{0.5}Bi_{0.5}TiO_3$, Ferroelectrics 6 (1986) 147.
[18] I.G. Siny, E. Husson, I.M. Beny, S.G. Lushnikov, E.A. Rogacheva, P.P. Syrnikov, A central peak in light scattering from the relaxor type ferroelectric $Na_{1/2}Bi_{1/2}TiO_3$, Physica B 293 (2001) 382.
[19] Elena Aksel, J.S. Forrester, Benjamin Kowalski, Marco Deluca, Dragan Damjanovic, J.L. Jones, Structure and properties of Fe-modified $Na_{0.5}Bi_{0.5}TiO_3$ at ambient and elevated temperatures, Physical Review B 85 (2012) 024121.
[20] Denis Schütz, Marco Deluca, Werner Krauss, Antonio Feteira, Tim Jackson, Klaus Reichmann, Lone-pair induced covalency as the cause of temperature and field induced instabilities in bismuth sodium titanate, Advanced Functional Materials 22 (2012) 2285.
[21] Chenggang Xu, Dunmin Lin, K.W. Kwok, Structure, electrical properties and depolarization temperature of $(Bi_{0.5}Na_{0.5})TiO_3$–$BaTiO_3$ lead-free piezoelectric ceramics, Solid State Sciences 10 (2008) 934.
[22] K. Ramam, S.H. Luis, Effect of Ba on ferroelectric and piezoelectric properties of the PLZT(1.2/55/45) system,, Physica Status Solidi 203 (2006) 2119.
[23] S.A. Nasser, Infrared absorption of some perovskite type titanates containing some additives, Journal of Materials Science Letters 9 (1990) 1453.
[24] J. Suchanicz, I.J. Sumara, T.V. Kruzina, Raman and infrared spectroscopy of $Na_{0.5}Bi_{0.5}TiO_3$–$BaTiO_3$ ceramics, Journal of Electroceramics 27 (2011) 45.
[25] Rachna Selvamani, Gurvinderjit Singh, Vasant Sathe, V.S. Tiwari, P.K. Gupta, Dielectric, structural and Raman studies on $(Na_{0.5}Bi_{0.5}TiO_3)_{1-X}(BiCrO_3)_X$ ceramics, Journal of Physics: Condensed Matter 23 (2011) 55901.
[26] Y.M. Li, W. Chen, Q. Xu, J. Zhou, X. Gu, S. Fang, Electromechanical and dielectric properties of $Na_{0.5}Bi_{0.5}TiO_3$–$K_{0.5}Bi_{0.5}TiO_3$ lead free ceramics, Materials Chemistry and Physics 94 (2005) 328.
[27] S. Shannigrahi, P.N.P. Choudary, H.N. Acharya, T.P. Sinha, Phase transition in sol–gel derived Na-modified PLZT ceramics, Journal of Physics D: Applied Physics 32 (1999) 1539.
[28] B. Andriyevsky, K. Dorywalski, I. Kityk, M. Piasecki, T. Lukasiewicz, M. Swirkowicz, A. Patrysn, J. Dec, N. Esser, C. Cobet, Spectral ellipsometry study on SBN single crystals in visible ultraviolet region, Ferroelectrics 147 (2011) 14.

[29] Xin-Yu Liu, Chang-Rong Zhou, Zhao-Hui Shan, Depolarization temperature and piezoelectric properties of $Na_{1/2}Bi_{1/2}TiO_3$–$Na_{1/2}Bi_{1/2}(Zn_{1/3}Nb_{2/3})O_3$ ceramics by two stage method, Bulletin of Materials Science 30 (2007) 579.
[30] Huidong Xie, Li Jin, Dezhong Shen, Xiaoqing Wang, Guangqiu Shen, Morphotropic phase boundary segregation effect and crystal growth in the NBT–KBT system, Journal of Crystal Growth 311 (2009) 3626.
[31] Bao-Jin Chu, Da-Ren Chen, Guo-Rong Li, Qing-Rui Yin, Electrical properties of $Na_{1/2}Bi_{1/2}TiO_3$–$BaTiO_3$, Journal of the European Ceramic Society 22 (2002) 2115.
[32] K. Uchino, S. Nomura, Critical exponents of the dielectric constants in diffused phase transition crystals, Ferroelectrics Letters 44 (1982) 55.
[33] G.A. Samara, Relaxational properties of compositionally disordered ABO_3 perovskites, Journal of Physics Condensed Matter 15 (2003) R367.
[34] D. Viehland, S.J. Jang, L.E. Cross, Freezing of the polarization fluctuation in lead magnesium niobate relaxors, Journal of Applied Physics 68 (1990) 2916.
[35] Z.Y. Cheng, L.Y. Zhang, X. Yao, Investigation of glassy behaviour of lead magnesium niobate relaxors, Journal of Applied Physics 79 (1996) 8615.
[36] R.R. Vedantam, V. Subramanian, V. Sivasubramanian, V.R.K. Murthy, Low frequency dielectric study of barium and strontium substituted $Pb(Zn_{1/3}Nb_{2/3})O_3$ ceramics, Japanese Journal of Applied Physics 42 (2003) 7392.
[37] B.K. Singh, Binay Kumar, Investigation of glassy behaviour of flux grown $Pb(Zn_{1/3}Nb_{2/3})0.91Ti_{0.09}O_3$ crystal, Physica B 406 (2011) 941.
[38] Z.Y. Cheng, R.S. Katiyar, Dielectric properties and glassy behaviour in the solid solution ceramics $Pb(Zn_{1/3}Nb_{2/3})O_3$–$PbTiO_3$–$BaTiO_3$, Philosophical Magazine B 78 (1998) 279.
[39] V.S. Tiwari, G. Singh, V.K. Wadhawan, Activation energy anomaly in the cluster dynamics of the relaxor ferroelectric $0.9Pb(Mg_{1/3}Nb_{2/3})O_3$–$0.1PbTiO_3$, Solid State Communications 121 (2002) 39.
[40] X.Y. Zhou, H.S. Gu, Y. Wang, W.Y. Li, T.S. Zhou, Piezoelectric properties of Mn doped $(Na_{0.5}Bi_{0.5})0.92Ba_{0.08}TiO_3$ ceramics, Materials Letters 59 (2005) 1649.